

NUMERICAL MODELS OF BOILING AND MIXING IN GEOTHERMAL WATERS

REED, MARK H. Department of Geological Sciences, University
SPYCHER, N. F. of Oregon, Eugene, OR 97403 USA
AKAKU, K. JAPEX, Geothermal Division, 2-17-22 Akasaka,
Minaoto-Ku, Tokyo, 107, Japan

Introduction

An accurate numerical model of the chemical processes involved in boiling of geothermal waters provides a basis for understanding the compositions of gases and boiled waters and for inferring the origins of scale in wells and surface equipment. Similar models of fluid-fluid mixing are useful for deducing the role of mixing in precipitation of scale and for determining the consequences to formation permeability of re-injection of processed geothermal waters. Here we report the application of computer programs CHILLER and SOLVEQ (Reed, 1982; Reed and Sycher, 1984, 1985) to modeling of boiling and mixing in geothermal waters from the Fushime System, Kyushu, Japan (Yoshimura et al, 1985; Akaku, 1988) and to Broadlands, New Zealand (Reed and Sycher, 1985). The Fushime system is particularly interesting because it is an excellent example of a saline high-T system that is precipitating lead and zinc sulfide minerals. The purpose of modeling boiling and mixing in the Fushime system is to understand the underlying chemical causes of scale precipitation from those waters and to understand the processes of epithermal ore formation from saline geothermal waters.

The numerical modeling consists of applying a Newton-Raphson technique to solve simultaneously a set of 30 to 50 equations that describe the following: a) Chemical mass balance for a set of thermodynamic components distributed among gases, minerals and aqueous species, b) Chemical equilibrium among phases and among components within phases, c) Enthalpy balance between gases and liquid. To model boiling, mixing, rock reactions, etc., this set of simultaneous equations is solved repeatedly with stepwise changes of temperature, pressure, enthalpy or composition between steps.

For the boiling and mixing calculations reported here, we applied the following enthalpy balance equation:

$$H_{\text{tot}} = \sum n_i H_i^l + \sum n_j H_j^g + dH \quad (1)$$

where H_{tot} is the total enthalpy of the system at the temperature and pressure of first boiling (e.g. 300 C, 86 bars); n_i and H_i^l refer, respectively, to the molar quantity and partial molar enthalpy of pure component i in the aqueous phase, and n_j and H_j^g refer to the corresponding quantities in the gas phase. The heat quantity, dH , is used to add or remove heat, as explained further below. The gas enthalpies for use in equation 1 are computed using the virial expressions of Sycher and Reed (1988).

The numerical treatments of complexing of aqueous ions, mineral equilibria, mineral solid solutions, and selection of mineral and gas phase assemblages are discussed in Reed (1982).

Reconstruction of the Deep Fushime Water

Some of the Fushime waters precipitate scales containing sulfide minerals and magnetite and some waters may have mixed with sulfate-rich waters causing anhydrite to precipitate. Mixing and scale formation, combined with boiling, change the primary water composition, making it necessary to compute a probable primary composition. Using analyses of Fushime liquid and gases collected at the surface (Yoshimura, et al, 1985) and a knowledge of the scale mineralogy (Akaku, 1988) and the alteration mineral assemblage at depth, the pH and other compositional properties of the deep water can be reconstructed. A quantity of the analysed gas phase, determined by assuming no excess enthalpy in the discharge, is recombined with the corresponding analysed aqueous phase as described by Reed and Sycher (1984).

In addition to recombining gas and liquid, initial concentrations of various metals were estimated in the primary liquid by computing forced equilibration (SOLVEQ) at 300 C of the gas-recombined water with minerals known or supposed to be in the alteration assemblage at depth (Yoshimura, et al, 1985). For Mg, Al, Mn, SiO_2 and Pb, the respective minerals used to compute their concentrations are: clinocllore, muscovite, rhodonite, quartz, and galena. Quantities of other metals were set relative to Pb in their proportions in analysed scale.

Boiling of Fushime SCG-1 water

For the purpose of simulating boiling effects in the Fushime system, we envision the following processes. Liquid phase enters the well at depth and begins to boil as it ascends. Boiling is assumed to be isoenthalpic, thus the quantity dH in equation 1 is set to zero throughout the P-T range of boiling. Boiling and consequent cooling result in precipitation of scale minerals, which fractionate from the liquid and gas from which they precipitated as the fluids move upward. The gas and liquid are assumed to remain in contact with each other throughout ascent. Except for quartz, chalcedony and cristobalite, whose precipitation we disallow, the computed scale mineral assemblage is that which is thermodynamically most stable.

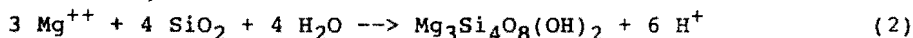
At temperatures above 175 C, the mineral assemblage produced by boiling is dominated by sulfides. The minerals to form include (Figure 1a) small quantities of magnesium and manganese silicates, but the dominant minerals are sulfides of Zn and Pb (sphalerite and galena) with lesser Cu sulfide (bornite). At 245 C, K-feldspar precipitates. The sulfides precipitate owing to the combined effects of the decreasing stability the chloride complexes of Cu, Pb, Zn and Fe (Figure 1c) with decreasing temperature and an increase in pH due to CO_2 degassing (see Figure 1b, pH changes from 5.44 at 300 C to 6.15 at 175 C). At 175 C, amorphous silica precipitates, and totally dominates the mineral assemblage at all lower temperatures, although sulfides continue to precipitate until boiling stops at 100 C. Much of the aqueous CO_2 and H_2S is partitioned into the gas phase initially, resulting in a rapid increase in pH near the beginning of boiling. This promotes abundant precipitation of sulfide minerals early in the boiling process.

The calculated bulk composition and phase assemblage of the mineral precipitates closely resembles those found in the Fushime wells and surface equipment, including the overwhelming abundance of Zn and Pb sulfides at high temperatures where boiling occurs, and the dominance of amorphous silica in lower temperature equipment. The precipitation of magnetite, observed in some wells at high temperature (Akaku, 1988) was not reproduced in the model calculations, for reasons that are not clear, but which relate, at least in part, to the inadequacy of thermodynamic data for Fe-Cl complexes at high temperature. Another possibility is that the natural waters may be enriched in iron by corrosion of steel equipment.

Mixing of Fushime SCG-1 water with Seawater

The boiling calculations show that an abundance of anhydrite that is observed above 1000 m in well SCG-1 (accompanied by Zn and Pb sulfides) cannot have precipitated owing to boiling. A reasonable possibility is that the anhydrite formed where warm or cold seawater (or seawater modified by reaction with wall rock) mixed with the ascending hot water. This hypothesis was investigated by a stepwise titration of warm seawater (100 C) into the numerical gas-liquid mixture computed at 275 C, at which temperature the two-phase mixture consists of 8.6 % gases (99.4% H_2O , 0.47% CO_2 , .012% H_2 , .092% H_2S , molal basis). An influx of the relatively cooler seawater must be heated initially by absorption of heat from the steam phase at constant T and P, until the steam is entirely resorbed, after which further addition of 100-degree seawater results in cooling of the whole mixture. The heat constraints on this process are modeled by applying the enthalpy balance equation in each step of the titration of warm seawater, setting the value of dH in equation 1 to the enthalpy of each increment of titrated seawater. Since we are interested in processes at a fixed point in space where the warm seawater mixes with hot hypogene water, the minerals are not fractionated from the system as they form, thus they are available to back-react as the seawater titration continues.

Addition of 174 grams of 100-degree seawater to an initial 1 kg. of the two-phase water (275 C) results in resorption of all of the gas (Figure 2b). The steam-heated mixture precipitates a large quantity of anhydrite (Figure 2c), owing to the retrograde solubility of anhydrite. The concentrated Mg^{++} in the seawater reacts with silica in the hot water, producing talc:



This reaction and a similar one for chlorite produces H^+ ion, causing the pH to decrease from 5.94 in the initial hot water to 4.78 in the mixed water (Figure 2d) at the point where all of the gas is resorbed. A separate mixing calculation using pure water indicates that approximately half of the pH drop

results from the resorption of CO_2 from the gas phase. The acidity of the mixed water precludes precipitation of sulfides while steam is being resorbed.

Once all steam is resorbed, further addition of warm seawater causes temperature to decrease (Figure 2a) and pH to increase to 5.44 after 8.7 kg of warm seawater has been added to the initial 1 kg of the hot water. The increase in pH results from "neutralization" of acid in the steam-heated water by the seawater (pH of seawater at 100 C is 6.0). The combined effects of increasing pH and decreasing temperature allow sulfide minerals to precipitate (Figure 2c), including sphalerite, galena, bornite, pyrite and cinnabar (HgS), producing an anhydrite-sulfide assemblage. The retrograde solubility of anhydrite causes it to dissolve as temperature decreases below 200 C. At 150 C, it is fully dissolved, leaving only sulfides and a small amount of barite in the mineral assemblage.

The anhydrite-sulfide mineral assemblage produced in the model mixing calculation closely resembles the scale observed in SCG-1, including the presence of magnesium and a small amount of silica, calculated to be in the form of talc. At equilibrium, reaction 2 depresses pH so much that sulfide mineral precipitation is impossible until temperature decreases substantially (Figure 2c). If talc fails to form fast enough to maintain equilibrium, pH would not decrease as much, and sulfides would precipitate at higher temperature, as found in a separate calculation of mixing with pure water. Amorphous silica was not computed to form, nor is it found in the anhydrite-bearing scale. It fails to form upon mixing because the dilution of aqueous silica by mixing outpaces the effect of cooling on decreasing the solubility of silica. The natural scale also includes small amounts of Hg, calculated to be in cinnabar, and Ba, in barite. It is apparent from the calculated precipitation of abundant anhydrite upon mixing of seawater with the hot geothermal water that in the natural geothermal system, there should exist a thick envelope of anhydrite filling pore volume at depth along the seaward recharge zone, perhaps resembling the anhydrite "alteration" described by Steefel (1987) in the Johnson River Zn-Pb-Cu District, Alaska.

Comparison to Broadlands

The preceding Fushime results will be compared to the Broadlands System, New Zealand, as modeled by Reed and Spycher (1985).

References

- Akaku, K., 1988, Geochemistry of mineral deposition from geothermal waters: Deposition processes of common minerals found in various geothermal fields and case study in the Fushime geothermal field. Chinetsu, in press.
- Reed M., 1982, Calculation of multicomponent chemical equilibria and reaction processes in systems involving minerals, gases and an aqueous phase, *Geochim. Cosmochim. Acta*, V. 46, p. 513-528.
- Reed, M.H., and N. Spycher, 1984, Calculation of pH and mineral equilibria in hydrothermal waters with application to geothermometry and studies of boiling and dilution, *Geochim. Cosmochim. Acta*, v. 48, p. 1479-1492.
- Reed, M.H., and N. Spycher, 1985, Boiling, cooling and oxidation in epithermal systems: A numerical modelling approach. Ch. 11 of Berger, B.R. and Bethke, P.M. (eds.), *Geology and Geochemistry of Epithermal Systems*, Reviews in Economic Geology, Volume 2, p. 249-272.
- Spycher, N.F. and Reed, M.H., 1988, Fugacity coefficients of H_2 , CO_2 , CH_4 , H_2O and of $\text{H}_2\text{O}-\text{CO}_2-\text{CH}_4$ mixtures: A virial equation treatment for moderate pressures and temperatures applicable to calculations of hydrothermal boiling. *Geochim. et Cosmochim. Acta*, 52, 739-749.
- Steefel, C., 1987, The Johnson River Prospect, Alaska: Gold-rich sea floor mineralization from the Jurassic. *Econ. Geol.* 82, 894-914.
- Yoshimura, Y., Yanagimoto, Y. and Nakagome, O., 1985, Assessment of the geothermal potential of the Fushime area, Kyushu, Japan. *Chinetsu* 22, 167-194.

Mineral abbreviations for figures 1 and 2 as follows: anhy, anhydrite (CaSO_4), bar, barite (BaSO_4), bn, bornite (Cu_5FeS_4); cc, chalcocite (Cu_2S); chl, chlorite; cinn, cinnabar (HgS); cp, chalcopyrite (CuFeS_2); cv, covellite (CuS); gn, galena (PbS); K-spar, potassium feldspar, py, pyrite (FeS_2); sl, sphalerite (ZnS).

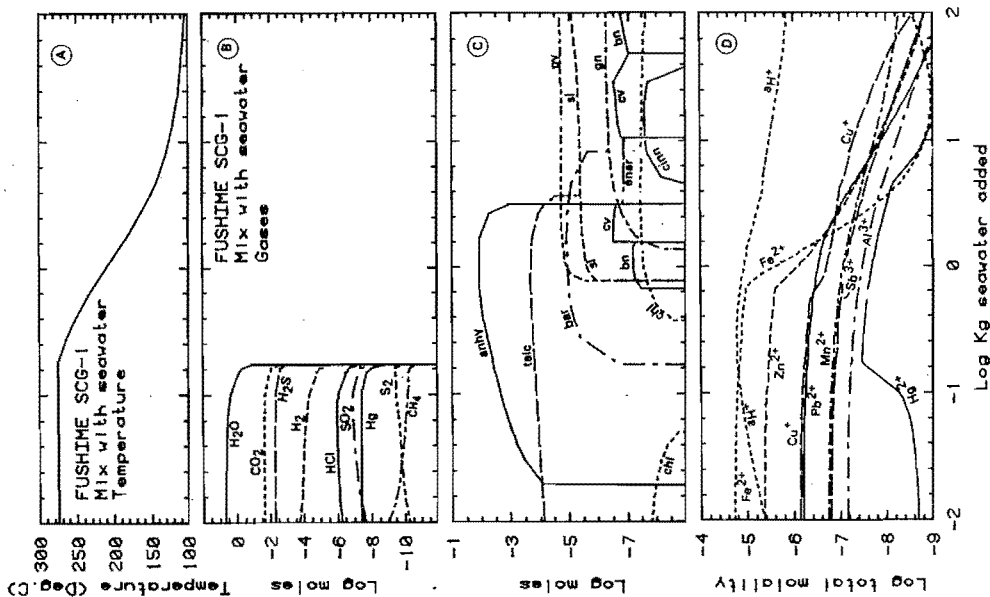


Figure 2. Results of numerical mixing of partly boiled fluid from Fushime well SCG-1. Boiling proceeds from right to left on figures. a) Mineral precipitates. b) pH (a_{H^+}) and total molality of metal component species. c) Molality of principal aqueous complexes of Cu, Zn and Pb. d) Molality of metal component species.

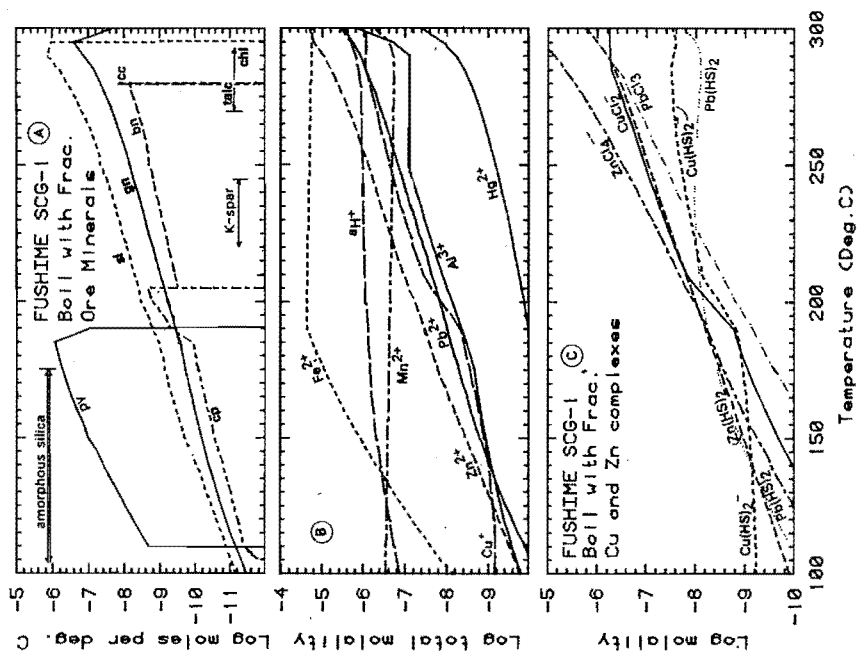


Figure 1. Results of numerical boiling of reconstructed fluid from Fushime well SCG-1. Boiling proceeds from right to left on figures. a) Mineral precipitates. b) pH (a_{H^+}) and total molality of metal component species. c) Molality of principal aqueous complexes of Cu, Zn and Pb.

GEOCHEMICAL MONITORING SYSTEM OF PRODUCTION WELL IN HATCHOBARU GEOTHERMAL AREA.

KOGA, A., UMEHARA, S., Geothermal Research Center, Faculty of Engineering,
Kyushu Univ., 6-1 Kasuga-koen, Kasuga 816, Japan
HIROWATARI, K., Kyushu Electric Power Co. Ltd., Fukuoka 810, Japan

INTRODUCTION

Chemical monitoring of production wells during exploration are used extensively in following changes that occur within a geothermal system, change in discharge characteristics, change with time, reinjection effect, etc.

If physical change such as temperature and pressure by dilution with other water, loss or gain of steam, reinjection, etc. take place in a geothermal system, changes occur in the discharging fluid chemistry. In other word, geochemical monitoring can be used to understand what happened or what will be happened in a geothermal system. Moreover, chemical monitoring has also the advantage of estimation of underground conditions in a geothermal system without disturbing the production wells. Thus, gathering of adequate geochemical records for each well in production play an important role in geothermal field management.

In Hatchobaru geothermal area, lots of geochemical data have been accumulated up to date during the period 1963-1988. This paper summarizes change in discharge characteristics and in fluid chemistry with time, effect of reinjection etc.

PRINCIPLE OF GEOCHEMICAL MONITORING SYSTEM

Trends in water solute concentrations within a field and changes with time are examined by chloride (a main anion constituent) in the deep water supplying the well versus by the water temperature calculated with silica method (or enthalpy obtained from the water and vapour discharging amounts). Figure 1 gives the trend lines which would be expected for various physical processes which may occur in the aquifer. [A] in the figure 1 is not the point, but a small area, showing the characteristics of the original deep water in a geothermal area. For various processes such as dilution, boiling condensation, evaporation, conductive loss or gain, reinjection, etc. We can, thus, interpret by geochemical monitoring what kind of processes happened in a geothermal system.

Figure 2 gives what is the percentage of chloride concentration in all anion constituent dissolving in the waters in some world-famous geothermal areas, showing that thermal waters discharging from the geothermal wells evaluated as the high Activity Index (Hayashi, et al. 1981) have characteristics of special chemical compositions such as over 90 % of $Cl/(Cl + SO_4 + HCO_3)$. However, the percentage is gradually decreasing by

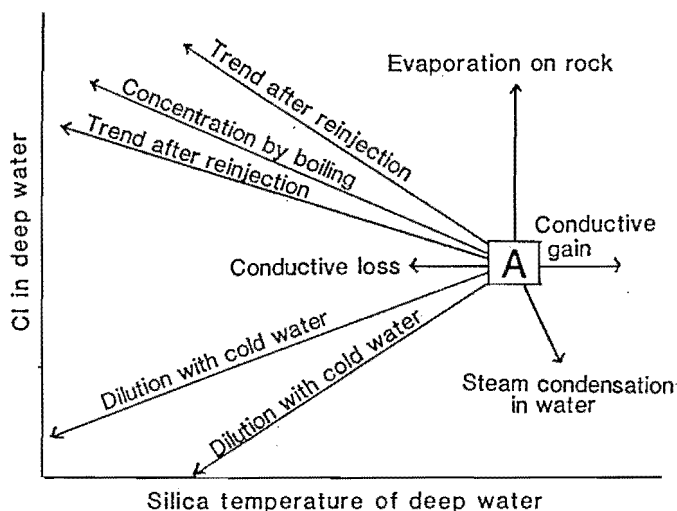


Fig.1 : Trend lines relating changes in deep-water chloride concentrations to various physical processes

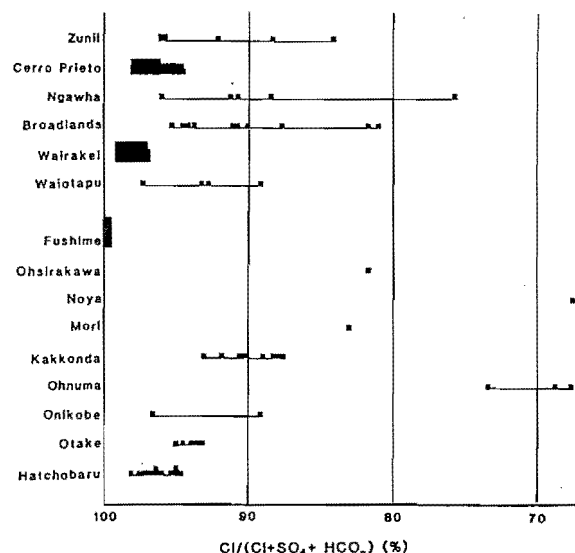


Fig.2 : $Cl/(Cl + SO_4 + HCO_3)$ % in some world-famous geothermal waters

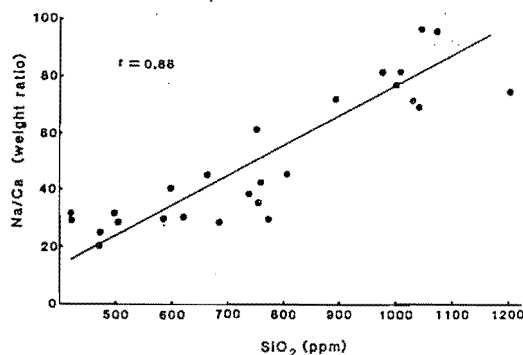


Fig.3 : Relationship between Na/Ca ratios and SiO_2 concentrations in Hatchobaru and Otake waters

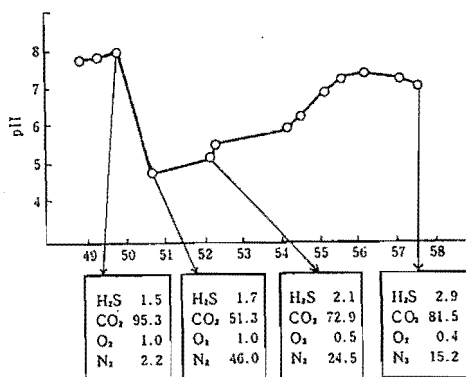


Fig.4 : Changes in gas compositions in steam and pH of Well 4 water with time

dilution with other water. Na/Ca ratios are also qualitatively high in high temperature waters. Sodium is the predominant cation and its concentration is not appreciably affected by changes in mineral equilibria. On the contrary, calcium in high temperature, neutral pH water is controlled by solubility of CaCO_3 , CaSO_4 and CaF_2 , which decreases in solubility with increasing temperature. Thus, Na/Ca ratios in deep thermal waters are high in proportion to the temperature as shown in Fig.3.

Not only chemical constituents in thermal water but gas compositions in steam also play an important role in geochemical monitoring. As an example Fig.4 gives the changes in gas compositions in steam and the pH of the water of Hatchobaru production well No.4. Since 1975, reinjection has started near the the well and air was also drawn into the aquifer. It caused the well to drop in pH of the water and change in gas composition in the steam respectively. Oxygen in the drawn air oxidizes H_2S to make H_2SO_4 , and so the N_2 content increased rapidly. Due to remove the reinjection well to other place, reinjection influence to well No.4 was gradually decreasing with time.

RESULT AND DISCUSSION

1) Changes in Cl concentrations and enthalpies with at Hatchobaru geothermal area

At Hatchobaru geothermal area, the initial chloride concentrations were originally 1500-1600 ppm, and the enthalpies of the well were 1200-1300 KJ/Kg, respectively, corresponding to [A] in Fig.1. Following exploration there were changes with time in the temperatures and chloride concentrations in individual wells. For many wells the following changes occurred during the production time.

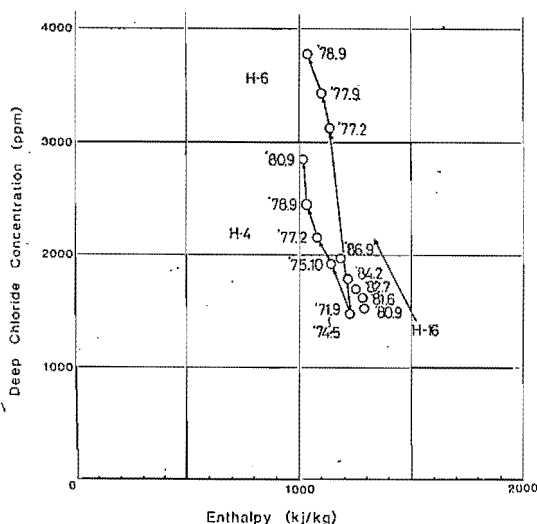


Fig.5 : Changes of Cl and enthalpy in some well waters (4,6,16) with time

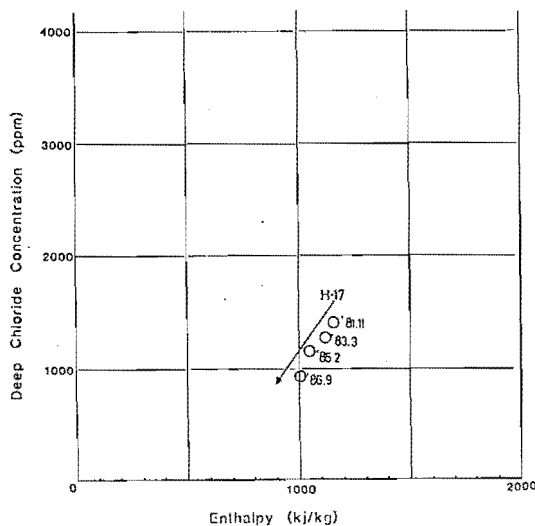


Fig.6 : Change of Cl and enthalpy in Well 17 water with time

a) Reinjection gave a big effect on the production wells. The chloride concentrations increased rapidly and enthalpy decreased slightly. Most of production wells followed on the line. Fig.5 shows examples of changes of Wells 4, 6, 16.

b) Both of Cl concentration and supply water temperature decreased with time. Fig.6 shows that the change of Well 17 is possibly out of the effect of reinjection and shows progressive dilution by a cold water during the period of observation.

c) If the steam condenses into reservoir, Cl concentration decreases and enthalpy increases. They are getting dry as shown in Fig.7 (Wells 10, 12, 13).

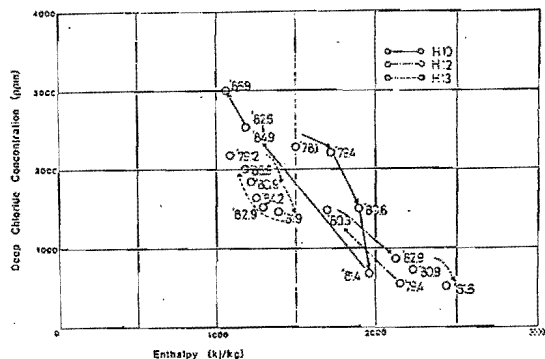


Fig.7 : Changes of Cl and enthalpy in well waters (10, 12, 13) with time

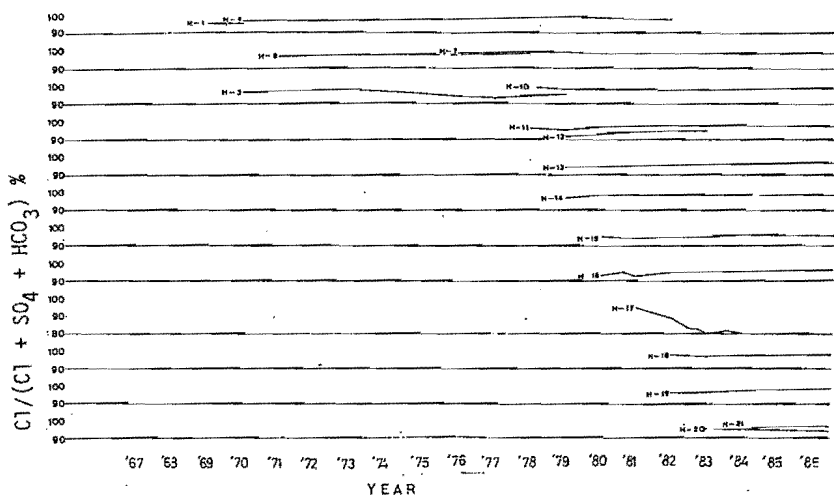


Fig.8 : Changes of $Cl/(Cl + SO_4 + HCO_3)$ % in well waters with time

2) Changes of $Cl/(Cl + SO_4 + HCO_3)$ ratios with time

Figure 8 gives the changes of $Cl/(Cl + SO_4 + HCO_3)$ ratios in the waters of production wells with time. The ratios are keeping about 95 % with time except Well 17, showing Hatchobaru is evaluated as a quite active geothermal area. Well 17 also started initially from 95 % but 2 years after the ratio became to 70 %, due to dilution with shallow water.

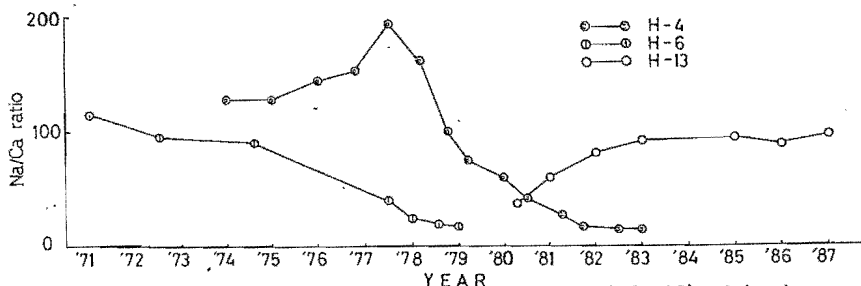


Fig.9 : Changes of Na/Ca ratios in well waters(4,6, 13) with time

3) Changes of Na/Ca ratios with time

From Figure 9 changes of Na/Ca ratios in Hatchobaru waters are divided into three categories;

a) Na/Ca ratios decrease with time : Well 6, 7, 11, 12, 14,15,16

b) Na/Ca ratios increase with time : Well 1, 13, 18, 20, 21

c) Na/Ca ratios firstly increase, then decrease : Well 3, 4, 17

Reinjection effect appears on the wells which indicate the decreasing Na/Ca ratios of the waters.

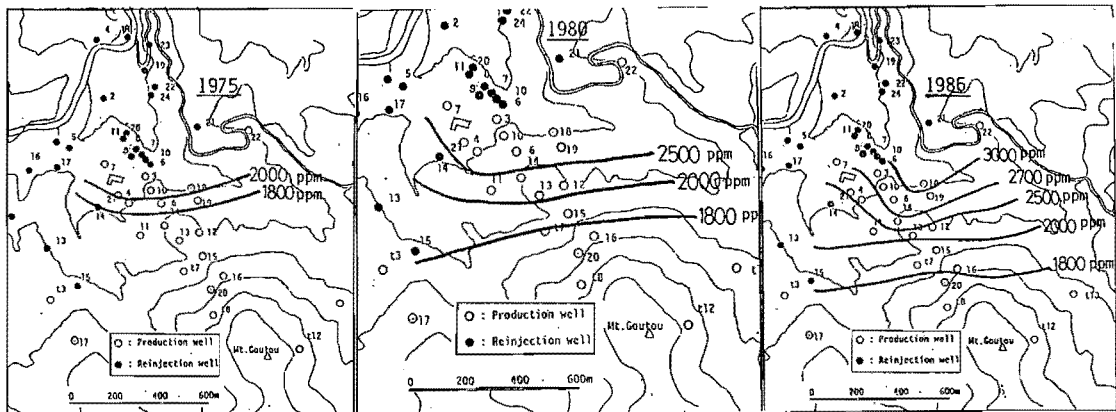


Fig. 10, 11, 12 : Changes of Cl concentrations in Hatchobaru waters with time ('75, '80, '86)

4) Increase of chloride concentrations in deep waters of the production wells by reinjection effect

Chloride concentration in Hatchobaru well was about 1600 ppm at the beginning of production time, but chloride concentrations were gradually increasing year by year due to injection effect. Their figures (Fig. 10, 11, 12) for Cl changes with time show that the rapid changes were observed during the period 1974 - 1978, but after 1979 the changes were getting small due to movement of reinjection wells.

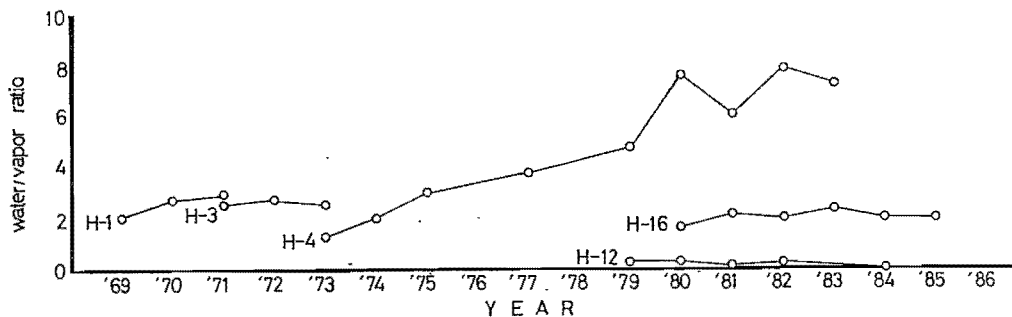


Fig.13 : Changes of water/vapor ratios in some wells (1,3,4,12,16) with time

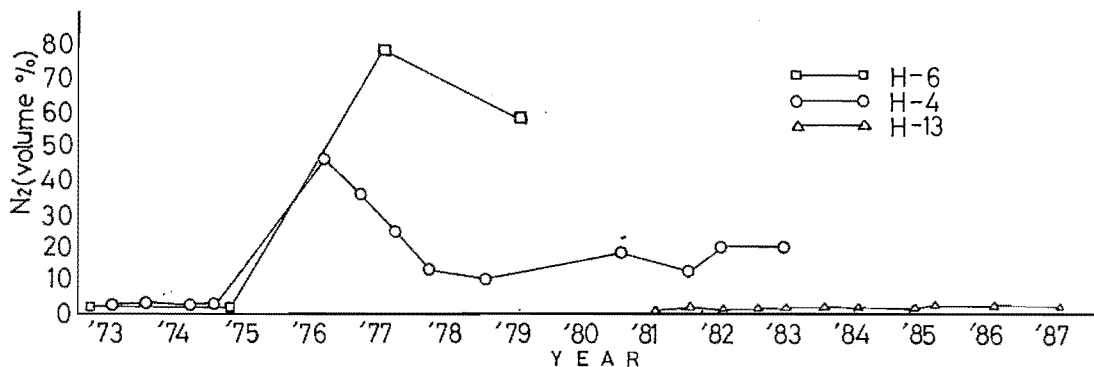


Fig.14 : Changes of N_2 gas contents in steam of wells (4,6,13) with time

5) Changes of water/vapour ratios and N_2 gas contents with time

Reinjection near production wells caused water/vapor ratios of wells to increase from 2-3 to 8 (Fig. 13). The increasing of the ratio gives decreasing of enthalpy, so we must keep it in my mind. On the other hand, Figure 14 gives as example the trends with time in N_2 gas contents in steam for some production wells. Well 4 and 6 were affected a lot by reinjection, whereas no effect for well 13.